Different mechanisms of cluster explosion within an unified time-dependent Thomas-Fermi approach: optical and short-wavelength regimes compared

Marian Rusek and Arkadiusz Orłowski
Institute of Physics, Polish Academy of Sciences, Aleja Lotników 32/46, 02–668 Warsaw, Poland
(Dated: October 27, 2004)

The dynamics of small ($\leq$ 55 atoms) argon clusters ionized by an intense femtosecond laser pulse is studied using a time-dependent Thomas-Fermi model. As follows from recent experiments, absorption of radiation and subsequent ionization of clusters observed in the short-wavelength laser frequency regime (98 nm) differs considerably from that in the optical spectral range (800 nm). Our theoretical approach provides an unified framework for treating these very different frequency regimes and allows for a deeper understanding of the underlying cluster explosion mechanisms. The results of our analysis following from extensive numerical simulations presented in this paper are compared both with experimental findings and with predictions of other theoretical models.

PACS numbers: 36.40.Gk, 32.80.-t, 52.50.Jm

I. INTRODUCTION

Clusters are agregates of atoms containing up to a few thousands atoms. Usually they are formed in expanding high-pressure gas jet. Atomic clusters have properties intermediate between those of an isolated atom and the bulk or solid-state material. The study of the interaction of such species with electromagnetic radiation is increasingly active research field. Clusters are as easily penetrated by a laser beam as gaseous media and, at the same time, exhibit large absorption of laser energy comparable to the solid targets [1].

Laser interaction with the atomic clusters differs substantially from that of simple atomic and molecular systems. Experiments on clusters irradiated by the intense laser pulses in the optical regime have revealed efficient generation of extremely highly charged atomic ions [2–8] and production of highly energetic particles (both electrons and ions), with kinetic energies of the MeV order [6, 7, 9–11].

Several theoretical models have been proposed to explain the mechanism underlying the production of highly charged energetic ions in interaction of atomic clusters with intense laser pulses with frequencies in the optical range. In classical Monte-Carlo simulations of cluster explosion the nuclei and unbound electrons are treated as classical particles obeying Newton's equations of motion [12–15]. The bound electrons are released with a certain probability depending on the electric field strength inside the cluster [12–15] and on collisions with other electrons and ions [13, 14].

Recently an application of the time-dependent density functional theory to a study of the response of atomic clusters to an intense laser pulse appeared [16]. A simplified one-dimensional model with frozen ion positions and the correlation effects neglected allowed to solve numerically time-dependent Kohn-Sham equations describing electron dynamics in a cluster. Results concerning the initial stage of ionization in moderate intensity regime were presented.

Intense short-wavelength radiation opens many new research areas in physics and chemistry. The photon energies in the vacuum ultraviolet (VUV) frequency range are large enough for the single photons to ionize irradiated matter. Since the binding energies of the electrons characterize individual elements, the ability to ionize matter allows direct insight into electronic structure and chemical composition of materials. On the other hand, the wavelength in the VUV regime is comparable to the atoms spacing in solids, and, therefore, the diffraction of short-wavelength radiation allows to determine the geometric structure of complex elements with atomic resolution.

Until now experiments were hindered by the lack of sufficiently intense short wavelength light sources. This situation is presently changing. Free-electron lasers making use of linear accelerators are expected to combine the advantages of synchrotron radiation (short-wavelength) with those of lasers (intense short pulses) and thus to pave the way to new types of experiments. Recently, the study of the interaction of intense VUV free-electron laser pulses with xenon [17] and argon [18] clusters has been reported.

It can be expected that the strong-field matter interaction in the short-wavelength VUV regime is considerably different from that at optical frequencies. The ponderomotive energy (average kinetic energy of a free electron oscillating in the radiation field) is a parameter that characterizes to some extent the interaction. For a typical optical pulse it reaches the values of several hundred eV whereas in the case of a short-wavelength pulse used in the DESY experiments [17, 18] it has a value of hundreds meV. Therefore field ionization, which is a dominant process in the optical domain, can hardly account for observations in the short-wavelength realm. Thus additional ionization and subsequent explosion mechanisms should be considered in the case of rare-gas atoms clusters exposed to the short-wavelength radiation [17].

At the first glance the well understood physics that the describes the laser pulse energy absorption by the cluster in the optical domain seems not to work in the frequency range used in the DESY experiments [17]. A standard

inverse bremsstrahlung model applied to the absorption of short-wavelength radiation by xenon clusters [17] predicted an absorption of only few photons per atom. This differs from the experimentally measured value by more than an order of magnitude.

In turned out that the problem was in the choice of the ionic scattering potential [19]. It seems that in a dense plasma formed by illuminating a xenon cluster with a VUV pulse the electrons experience more than just a Coulomb potential. By using Yukawa-like form of the screening potential the authors of [19] have shown that their implementation of inverse bremsstrahlung model is able to reproduce the large number of VUV photons observed in the experiment [17].

Similar situation occurs in the case of the argon clusters irradiated by a short-wavelength laser pulse. In a recent experiment [18] each argon atom in the cluster absorbed on average up to 20 photons while losing 2 electrons. Also in this case the standard collisional heating model cannot fully account for the strong laser energy absorption.

In this paper we further extend and refine a time-dependent Thomas-Fermi model introduced in our previous paper [20] to describe the dynamics of argon clusters in an intense laser pulse. Both optical *and* short-wavelength regimes are analyzed and the explosions mechanism are compared. A simplified one-dimensional version of a similar model has been already successfully applied to the description of cluster explosion in optical frequency regime [21, 22]. In our previous work a three-dimensional model produced promising results for argon atoms and 6 atom argon clusters subjected to an optical pulse [20]. The slightly refined version of the model allowed us to extend these previous results to a more realistic case of 55 atom cluster in three-dimensions [23]. This new version of the model permits us also to attack the short-wavelength case (for a preliminary numerical evidence see [24]). In the present paper we go much further by analyzing the realistic case of larger clusters, providing a synthetic physical interpretation encompassing both cases. The results obtained in the present paper look very promising and seem to agree with the experimental findings [18].

Note that the time-dependent Thomas-Fermi model used automatically yields a Yukawa-type screening of the Coulomb potential used in [19]. This was shown in our previous paper [20] in the case of a simplified relation of the internal energy of the electron gas (ρ^2 instead of $\rho^{5/3}$). Our theoretical treatment does not require the assumption of thermodynamical limit used in [19] and thus does not limit us to the study of "sufficiently large" clusters. Also the perturbation theory is no longer needed which allows us in principle to go to the higher intensities where nonlinear effects may arise.

This paper is organized as follows. In Section II the time-dependent Thomas-Fermi model is introduced. Then in Section III the details of numerical calculations are presented. In section IV we check the results coming from the model in the optical frequencies regime. Main results concerning short-wavelength pulses are described in Section V. Finally we finish with a brief summary.

II. THEORETICAL MODEL

The Thomas-Fermi model introduced in the mid 1920's by Thomas [25] and independently by Fermi [26] embodies many of the features of the modern density functional methods [27, 28]. Within this model the ground state structure of an atomic cluster is described by the average electron density $\rho(\vec{r})$ and the positions of the nuclei $\vec{R}_a$. It can be obtained by minimization of the following Thomas-Fermi energy functional $\mathcal{E}_{\rm TF}$ which is a sum of the internal and potential energies [20]:

$$\mathcal{E}_{\rm TF} = \mathcal{E}_{\rm int} + \mathcal{E}_{\rm pot} \tag{1}$$

In the equation above the relations for the internal (kinetic) energy $\mathcal{E}_{\rm int}$ of an ideal electron gas at temperature $T = 0$ are used locally:

$$\mathcal{E}_{\rm int} = c_k \int d^3r \, [\rho(\vec{r})]^{5/3}, \quad c_k = \frac{3}{5}\frac{\hbar^2}{2m}[3\pi^2]^{2/3} \tag{2}$$

and the potential energy $\mathcal{E}_{\rm int}$ of mutual Coulomb interactions of electrons and nuclei is given by:

$$\mathcal{E}_{\rm pot} = \frac{e}{2}\int d^3r \, \left[\sum_{a=1}^{N} Z\,\delta(\vec{r}-\vec{R}_a) - \rho(\vec{r})\right] \Phi(\vec{r}) \tag{3}$$

where the self-consistent Coulomb potential $\Phi(\vec{r})$ reads as:

$$\Phi(\vec{r}) = e\int \frac{d^3r'}{|\vec{r}-\vec{r'}|}\left[\sum_{a=1}^{N} Z\,\delta(\vec{r'}-\vec{R}_a) - \rho(\vec{r'})\right]. \tag{4}$$

Here N is the number of atoms in the cluster, e is the elementary charge, and m denotes the electron mass.

The collective Thomas-Fermi model is most valid for heavy atoms — with many electrons. It has been used for the calculation of ionization potentials of different atomic numbers and ionization degrees [29]. In this paper we use the time-dependent version of the Thomas-Fermi model to describe ionization of argon atoms (atomic number $Z = 18$). Even for such a relatively low value of Z the ionization potentials calculated in [29] agree well with real values in some range of ionization degrees (at low ionization degrees the method breaks down because of the lack of exchange, while for high degrees only a few electrons remain and the statistical Thomas-Fermi approach stops to work). This is confirmed in [30] where multiphoton ionization of noble gases atoms in strong laser field is explained theoretically using the Thomas-Fermi model. The results compare favorably with experiments.

To introduce a time-dependent version of the Thomas-Fermi model we assume that the electron density at any

point of space is obtained by summing up the contributions from n smoothed pseudo-particles [20]:

$$\rho(\vec{r}) = \frac{Z\,N}{n} \sum_{j=1}^{n} f_j(\vec{r} - \vec{r}_j) \tag{5}$$

(the functions f_j are assumed to be normalized $\int d^3r f_j(\vec{r}) = 1$).

The dynamics of the electron density (5) and the motion of the nuclei is governed by the following Hamiltonian in which the Thomas-Fermi energy functional (1) plays a role of the potential energy term [20]:

$$\mathcal{E} = \mathcal{E}_{\rm kin} + \mathcal{E}_{\rm TF} \tag{6}$$

and the kinetic energy (of translational motion) of electrons and nuclei reads as:

$$\mathcal{E}_{\rm kin} = \sum_{a=1}^{N} \frac{M\,\vec{V}_a^2}{2} + \int d^3r\,\rho(\vec{r})\,\frac{m\,[\vec{v}(\vec{r})]^2}{2} \tag{7}$$

(M denotes the nuclear mass).

After inserting Eq. (5) into Eq. (6) and assuming that the functions f_j are sufficiently δ-like (i.e., neglecting terms of the second order in characteristic width of the kernel functions f_j [31, 32]) one arrives at the following Hamilton equations of motion for the smoothed pseudo-particles positions $\vec{r}_j$ (c.f., [20]):

$$m\,\frac{d^2\vec{r}_i}{dt^2} = -\frac{2}{3}\sum_{j=1}^{n}\left(\frac{c_k}{\rho_i^{1/3}} + \frac{c_k}{\rho_j^{1/3}}\right)\vec{\nabla}_i w_{ij}(\vec{r}_i - \vec{r}_j) + e\,\vec{\nabla}_i\Phi_i \tag{8}$$

where

$$w_{ij}(\vec{r}) = \frac{Z\,N}{n}\int d^3r'\,f_i(\vec{r'} - \vec{r})\,f_j(\vec{r'}) \tag{9}$$

and the transition between field quantities $F(\vec{r})$ ($F = \rho, \vec{v}, \Phi, \ldots$) and pseudo-particle-based quantities F_i is done in the following way:

$$F_i = \int d^3r\,f_i(\vec{r} - \vec{r}_i)\,F(\vec{r}) \tag{10}$$

Equations (8) can be understood as a discretized Smooth Particle Hydrodynamics [33, 34] version of the Bloch-like hydrodynamic equations [35]. Therefore, by treating the Thomas-Fermi energy functional as a potential energy part of the Hamiltonian of the system we had viewed the oscillations of the electron cloud in an atomic cluster as a motion of a fluid characterized by a density $\rho(\vec{r}, t)$ and a velocity field $\vec{v}(\vec{r}, t)$. A similar hydrodynamic model has been used in the weak-field limit to study photoabsorption of an atom in free space [36] and in plasma [37]. Also multiple ionization of xenon atoms by a strong laser field was studied using a two-dimensional version of a similar model [38].

The hydrodynamic equations for the electron density ρ are supplemented by the Newton-like equations of motion for the positions of the nuclei $\vec{R}_a$:

$$M\,\frac{d^2\,\vec{R}_a}{d\,t^2} = -Ze\vec{\nabla}\Phi(\vec{R}_a). \tag{11}$$

The interaction with the laser pulse is treated within the dipole approximation by replacing the electrostatic Coulomb potential in Eq. (4) by:

$$\Phi(\vec{r}) \to \Phi(\vec{r}) - \vec{r}\cdot\vec{\mathcal{F}}, \tag{12}$$

where $\vec{\mathcal{F}}$ is the electric field of the incoming wave. The linearly polarized wave of a pulse used in the simulations is assumed to have a field envelope proportional to sine squared with a full width at half maximum τ and an optical period τ_0:

$$\vec{\mathcal{F}}(t) = \vec{\mathcal{F}}_0\,\sin^2\left(\frac{\pi}{2\tau}\,t\right)\cos\left(\frac{2\pi}{\tau_0}\,t\right) \tag{13}$$

Note, that the theoretical approach presented here includes several possible ionization mechanisms: above-the-barrier (or field) ionization both by an external laser field, and by an internal field due to the space-charge distribution inside the cluster, as well as (to some extent) electron-impact (or collisional) ionization.

III. CALCULATION DETAILS

The electron density in a neutral Thomas-Fermi atom is singular at the nucleus. At large distances from the nucleus r it falls off as r^{-6} rather than exponentially [39]. An electron cloud of an ion has a finite cut-off radius. In order to model the electron density of Thomas-Fermi atoms and ions as a sum of smoothed pseudo-particles (5) one should in principle use a variable pseudo-particle width: narrower pseudo-particles to model the electron cloud in the vicinity of the nucleus, and wider pseudo-particles to model the outer shells of the atom (or ion).

In our previous paper [20] we utilized f_j from Eq. (5) in the form of a Gaussian function *identical* for all pseudo-particles:

$$f(\vec{r}) = \left(\frac{\alpha}{\sqrt{\pi}}\right)^3 e^{-(\alpha\,\vec{r})^2}. \tag{14}$$

It turned out however that this choice of fixed width of all pseudo-particles leads to some problems in modeling the electron cloud close to the nucleus. Several pseudo-particles were stacking atop on each other and the Smooth Particle Hydrodynamic method used was breaking down. To prevent this we have chosen a large value of the parameter α ($\alpha = 7$ for $Z = 18$ and $n/N = 125$) from Eq. (14). That choice increased the maximum force appearing in the simulations, what in turn made the numerical code extremely slow and turned any realistic calculations nearly impossible.

Let us stress that the condition of validity of the Thomas-Fermi theory is not well obeyed near nuclei where the singular Coulomb potential varies rapidly over a characteristic electron wavelength. Therefore instead of modeling the electron cloud close to the nucleus with a large number of test-particles of very small width we made a more physical choice – the electron density of an atom is modeled by test-particles of two kinds: one large particle originally centered at the nucleus which represents the core electrons and a large number of smaller particles modeling the outer shells of an atom:

$$\rho(\vec{r}) = \frac{Z\,N}{n}\left\{\xi\left[\sum_{j=1}^{n} f(\vec{r}-\vec{r}_j)\right] + (1-\xi)\,\frac{n}{N}\,g(\vec{r}-\vec{r}_0)\right\}, \tag{15}$$

where f is given by Eq. (14) and

$$g(\vec{r}) = \left(\frac{\beta}{\sqrt{\pi}}\right)^3 e^{-(\beta\,\vec{r})^2}. \tag{16}$$

We have chosen $\beta = 1/r_0$ where r_0 is the radius of the Thomas-Fermi ion of charge $Z(1-\xi)$ (i.e., $Z\xi$ electrons remain to be bound) [40]:

$$r_0 = 3.17361\,\frac{\sqrt{(1-\xi)/\xi}}{Z^{1/3}}. \tag{17}$$

The parameter α from Eq. (14) was chosen to model well an isolated Thomas-Fermi atom of given Z [20]. For this value of α the Thomas-Fermi energy relations are preserved [39]:

$$2\,\mathcal{E}_{\rm int} + \mathcal{E}_{\rm pot} = 0 \tag{18}$$

This choice was done in the following way. First ground states of an atom corresponding to several different values of α were prepared. It turns out that the relation (18) holds only for a certain value of α which was than used to model the interaction of the cluster with the laser pulse. For example for $n/N = 125$ pseudo-particles per atom (this is the value used later in the paper), and $Z = 18$ (argon atoms) we have found $\alpha = 5$ for $\xi = 0.1$ and $\alpha = 1.5$ for $\xi = 0.5$.

Let us mention that because the collective Thomas-Fermi model is basically statistical in nature, it cannot be applied directly to the low electron density regions, as in the outer shells of the neutral atom. By modeling the electron density of an atom by a *finite* number of pseudo-particles we in fact introduce some cut-off radius and these low density regions are not considered. By changing the parameter ξ from Eq. (15) we can manipulate the value of this cut-off and chose how well the outer shells of an atom should be modeled. For example in the case of $\xi = 0.1$ (and $\alpha = 5$) the cut-off radius is small, and therefore the outer shells are not well modeled. In the second case of $\xi = 0.5$ (and $\alpha = 1.5$) the cut-off radius is larger, and therefore the outer shells are modeled better (at the expense of the core electrons which in this case are represented by a single Gaussian function).

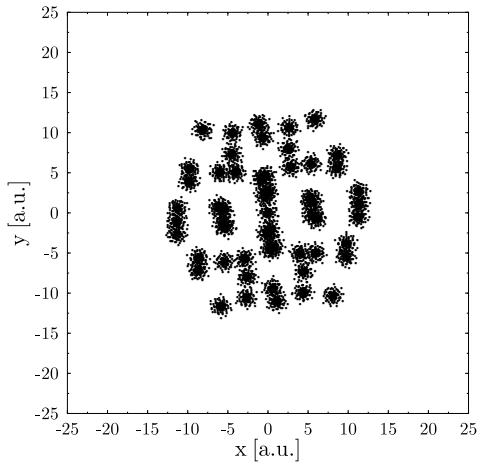

FIG. 1: Ground-state structure of a $N = 55$ atom cluster with $\xi = 0.1$. Equilibrium positions of the nuclei $\{\vec{R}_a\}$ are marked by filled circles. Small black dots correspond to the positions of the pseudo-particles modeling the equilibrium electronic density ρ.

Ground state properties of small clusters of rare-gas atoms have been investigated extensively in the literature (see, e.g., [41–44]). The usual theoretical approach is to describe the atoms in a cluster as a system of particles interacting via a short-range potential such as, e.g., the Lennard-Jones potential. It has been reported that particularly stable configurations of such clusters are of the form of closed-shell icosahedron. For example a $N = 55$ atom cluster consists of two icosahedral shells and one atom in the middle; the second shell can be separated into two sub-shells with different radii.

We downloaded from [45] the publicly available ground state structures of $N = 55$ atom Lennard-Jones clusters and used them as the equilibrium positions of the nuclei in the Thomas-Fermi model. The positions of the nuclei were rescaled so that equilibrium distance between two atoms is $R_0 \simeq 7\,[\text{a.u.}] = 3.7\,\text{Å}$ which is similar to the spacing of atoms in argon clusters [46]. Next they were used as an input into the hydrodynamic calculations involving the motion of an electron fluid. The resulting example ground-state structures are shown in Figs. 1 and 2. Let us note that in Fig. 1 the electron clouds of individual atoms are well separated. On the contrary, in Fig. 2 we observe the larger radius of the pseudo-particles as compared to Fig. 1. This allows us to model the electron cloud in between the atoms with greater accuracy.

Notice that, as shown by [47], additional corrections are needed to the Thomas-Fermi functional in order to model inter-atomic bonds. However it turned out that in the case of a cluster illuminated by a short 100 femtosecond pulse considered in this paper, the ground-state structure of a cluster obtained by a minimization of the

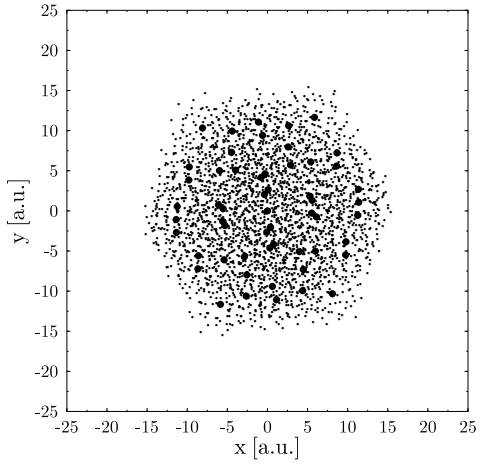

FIG. 2: Ground-state structure of a $N = 55$ atom cluster with $\xi = 0.5$. Equilibrium positions of the nuclei $\{\vec{R}_a\}$ are marked by filled circles. Small black dots correspond to the positions of the pseudo-particles modeling the equilibrium electronic density ρ.

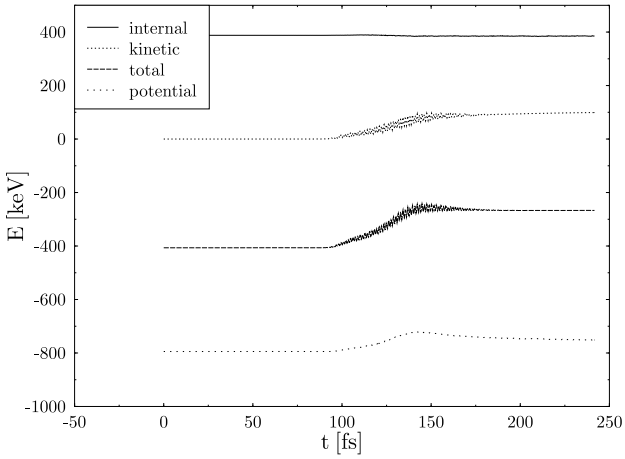

FIG. 3: Potential, kinetic, internal and total energy of an 55 atom argon cluster illuminated by a laser pulse plotted versus time. The Thomas-Fermi energy relations are preserved at the initial time. Total energy absorbed from the laser pulse is clearly visible. Efficient laser energy absorption starts when the pulse envelope approaches its maximal value.

standard Thomas-Fermi functional turned out to be stable enough during the time of interest.

In the next step we make use of the two obtained ground states to proceed with the simulations. We are concerned with the interaction of the laser pulses with these clusters.

IV. INFRARED PULSE

Let us first check how well our model works in the optical frequency domain. The ground-state cluster structure from Fig. 1 will be now illuminated by a typical laser pulse of infrared frequency (a similar pulse was used, e.g., in the experiments by [48]). The atoms of the cluster have initially no kinetic energy and are subject to an oscillating electric laser field at intensity $I = 1.4 \times 10^{15}\,\frac{\mathrm{W}}{\mathrm{cm}^2}$ (or $\mathcal{F}_0 = 0.2\,[\mathrm{a.u.}]$). The pulse used in the simulations had a wavelength $\lambda = 800\,\mathrm{nm}$ and a temporal full width at half maximum $\tau = 106.67\,\mathrm{fs}$ (or $\tau/\tau_0 = 40$). The electric field of the pulse was polarized linearly along the x axis. The same pulse parameters were used in our previous paper [20] (where only a 6 atom cluster was studied).

In Fig. 3 we plot the internal (2), potential (3), kinetic (7) and total energy of an 55 atom argon cluster illuminated by a laser pulse plotted versus time. It is seen that the Thomas-Fermi energy relations are preserved at the initial time, i.e., the potential energy is twice as large as the internal energy with the minus sign as in Eq. (18). At later times the electric field of the laser becomes strong enough to start above the barrier ionization of the cluster atoms (tunnel ionization which may happen at lower values of the field is not described by our semiclassical model). Thus inner ionization starts. The electrons released from the individual atoms still remain bounded by the cluster as a whole. Next they are ejected from the cluster by the still increasing pulse (outer ionization) and start to oscillate in the electric field of the laser. As seen from inspection of Fig. 3 this happens at $\simeq 80\,\mathrm{fs}$: at this time the oscillations of the total kinetic energy become visible. These laser driven electrons are effectively heated through collisions with the cluster ions (inverse bremsstrahlung). It follows from Fig. 3 that such an efficient laser energy absorption starts when the pulse envelope approaches its maximal value. This absorbed energy is then converted into translational energy of the ions and cluster disintegrates by a Coulomb explosion process. At the end of the pulse the kinetic energy of the ions grows at the expense of the potential energy and the total energy remains constant. Thus the total energy absorbed from the laser pulse is clearly visible.

In Fig. 4 we present the structure of the cluster just after the pulse is finished. The size of the cluster is more than ten times larger than the ground state structure from Fig. 1. An inset shows the electron cloud at a $1:100$ magnification (i.e., the x and y coordinates vary from -30000 to $30000\,[\mathrm{a.u.}]$.) It is seen that the electrons are ejected mainly along the pulse polarization axis (i.e., along the x axis).

It follows from inspection of Fig. 4 that almost all free electrons were removed from the cluster by the laser pulse. This observation makes the calculation of the charges of the outgoing ions feasible. They were calcu-

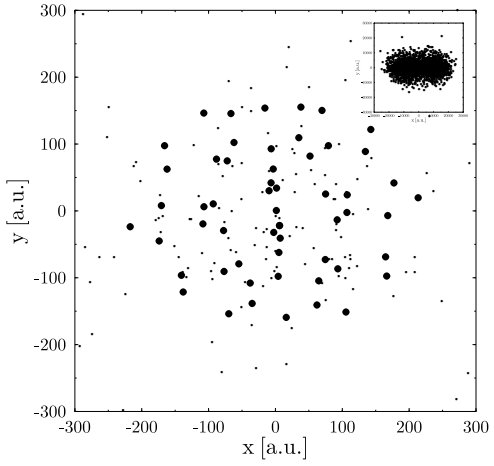

FIG. 4: Excited $N = 55$ atom cluster from Fig. 1 the end of the laser pulse at $t = 250$fs. Positions of the nuclei $\{\vec{R}_a\}$ are marked by filled circles. Small black dots correspond to the positions of the pseudo-particles modeling the electronic density ρ. An inset shows the electron cloud at a $1 : 100$ magnification (i.e., the x and y coordinates vary from -3000 to 3000 [a.u.].)

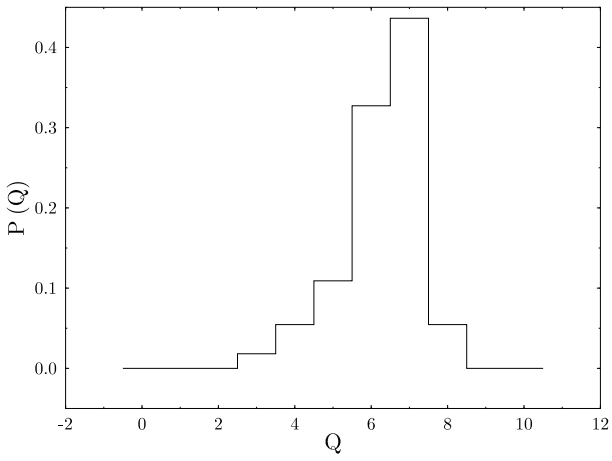

FIG. 5: Distribution of the final charges of the ions formed in the explosion of an 55 atom cluster. They agree with both experimental results and recent theoretical predictions.

lated in the following way: for each pseudo-particle its charge is added to the charge of the closest ion; pseudo-particles which are further from any ion than 10 [a.u.] are considered lost. In Fig. 5 we plot the resulting distribution of the final charges of the ions formed in the explosion of the cluster. Charges as high as 8^+ are observed. The results are consistent with both experimental results by Purnell [48] and theoretical predictions by Ishikawa [12]. It is seen from inspection of Fig. 5 that it is not possible to tell from which shell of the cluster an ion is coming just by looking at its charge. What we need is both charge *and* kinetic energy.

Thus in Fig. 6 we have the kinetic energy of the ions plotted as a function as the charge state. Small dots correspond to individual ions while larger filled circles represent results averaged over (sub)shells. The linear dependence of the ion energy on ion charge seems to be a good approximation for each (sub)shell. For argon clusters Coulomb repulsion is the key explosion mechanism [8]. Thus ion energy should have a quadratic dependence on ion charge [1, 7]. As shown theoretically by Ishikawa [12] (who also observed linear dependence for given shells) it is possible to get the experimentally observed quadratic dependence by summing contributions from different cluster shells and/or different laser intensity regions.

Note that the ions coming from the outer shells of the cluster (leaving the cluster first) are more energetic than those coming from the inner shells (leaving the cluster later). Such a stepwise character of the explosion has been suggested as an explanation of phenomena observed in experiments [8] and confirmed within 1D numerical simulations using a similar time-dependent Thomas-Fermi hydrodynamic model [21] as well as with our previous simulations [20].

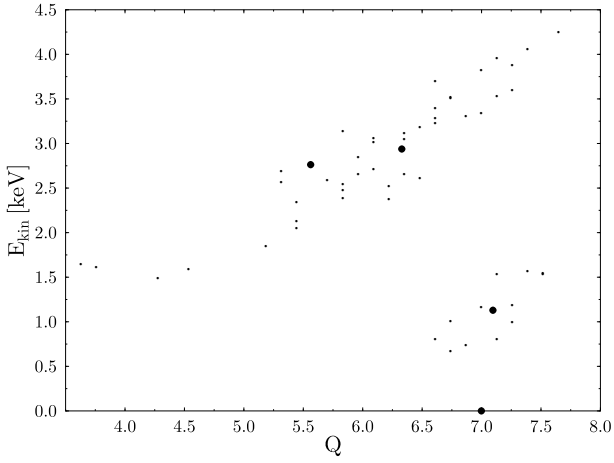

FIG. 6: Kinetic energy of the ions plotted as a function as the charge state. Small dots correspond to individual ions while larger filled circles represent results averaged over (sub)shells. The linear dependence of the ion energy on ion charge seems to be a good approximation for each (sub)shell.

Therefore from Fig. 6 we conclude that the most ionized atoms come from the inner shells of the cluster. This shows the dependence of atomic ionization rates on the

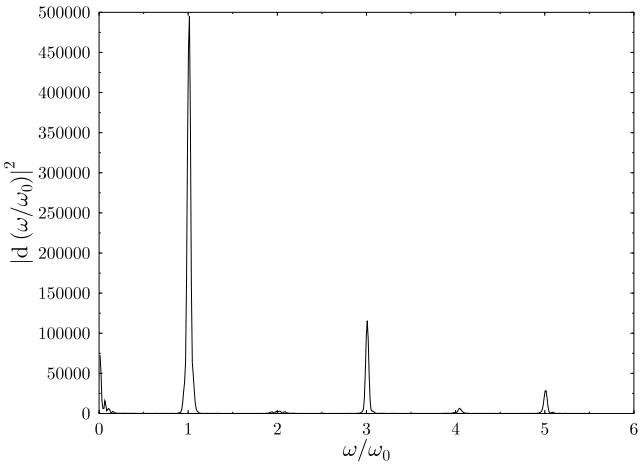

FIG. 7: Radiation spectrum of the cluster plotted as a function of the frequency relative to the frequency of the laser pulse. Odd harmonics are generated during the cluster explosion process. The spectrum falls off for the first harmonics (later a plateau is expected).

original position of an atom in the cluster and is in agreement with results of the 1D TDFT simulations [16]. Let us present a following explanation of this observation. Field ionization induced by an external laser field starts at the same time for all atoms of the cluster. Next the ionization of the inner shell seems to be slowed down by the presence of the outer shells of the cluster. At later times the outer shells explode and ionization of the inner shell is strongly enhanced by electron impact ionization due to the laser field driven oscillations of the electrons liberated from the cluster atoms. Since these electrons oscillate mainly along the linear polarization axis of the laser pulse, they do not affect the outer shells of the cluster, which are already far away from the original position of the cluster.

One of the main motivations behind the laser-cluster interaction studies was probably the desire to generate photons with energies much larger than the energy of a single laser photon. One of the possible high-energy photon generation mechanism is the high order harmonic generation in strong laser fields. Note that due to the nonlinearity inherent in the Thomas-Fermi model it is also possible to see some traces of this effect in our simulations. We have calculated the dipole moment d of the cluster from Fig. 1 illuminated by a infrared laser pulse. Its squared Fourier transform is plotted in Fig. 7 as a function of the frequency. We see that odd harmonics of the incoming wave are generated during the cluster explosion process (the generation of even harmonics requires particular spatial symmetry of the nonlinear medium). This will be contrasted with the short-wavelength case.

Let us mention, that we have also tried to explode the second ground-state structure from Fig. 2 using the same infrared laser pulse. However in this case the results we had got are unphysical. Indeed in the case of $\xi = 0.5$ as much as 9 core electrons are modeled by a single Gaussian particle. For a high ionization degrees (c.f., Fig. 5) this leads to wrong results: at the end of the pulse each atom was ionized only 4 times. Thus the dynamics of the core electrons seems to play an important role in the cluster explosion at optical frequencies.

V. ULTRAVIOLET PULSE

Encouraged by reasonable results coming out from the time-dependent Thomas-Fermi model in the optical frequencies regime we would like now to apply it to the description of DESY experiments with argon clusters [18]. In these experiments small (≤ 900 atoms) argon clusters were illuminated by a focused free-electron laser radiation at a power density up to $10^{14}\,\mathrm{W/cm^2}$. At such a high power density the absorption and ionization of argon clusters with VUV radiation turns out to be independent of the wavelength and the specific electronic structure of the cluster [18]. Thus the semiclassical Thomas-Fermi model seems to be a reasonable choice in this intensity regime.

At 98 nm laser wavelength the energy of a single photon is 12.7 eV. Since the ionization potential of Ar atoms is 15.5 eV, at least two photons were needed to ionize each atom. The laser energy absorption in a cluster is strongly enhanced. In a cluster each Ar atom absorbs up to 20 photons and loses on average 2 electrons.

Let us first illuminate by a short-wavelength pulse of ultraviolet frequency the 55 atom argon cluster ground state from Fig. 1. The pulse used in the simulations had a wavelength 98 nm (or $\tau_0 = 13.527$[a.u.]), temporal full width at half maximum of 50 fs (or $\tau/\tau_0 = 150$), and the peak intensity of $10^{14}\,\mathrm{W/cm^2}$ (or $|\vec{\mathcal{F}}_0| = 0.05$ [a.u.]). It turns out that in this case there is practically no laser energy absorption. The clusters survive the pulse intact and no atoms get ionized.

We conclude that the vibrations of the core electrons that were well modeled in the optical case are not relevant. They eventually could start playing a role at higher VUV pulse intensity, as suggested in [49], where a simple man's (one dimensional) model was used. We proved, however, that in the intensity regime considered in this paper, even more sophisticated 3D not-that-simple man's model, does not help in explaining the strong energy absorption observed in experiments.

One possible source of this problem may be the fact that the Thomas-Fermi model works well only in a certain ionization degrees regime. Indeed the authors [29] studied ionization potentials of different atoms using the Thomas-Fermi model. In the case of $Z = 20$ (a Z number close to 18 for argon) and ionization degrees $\propto 0.1$ (close to the experimental result) the ionization potential coming from the model is overestimated by factor of 3.

Another possible reason for the discrepancy between theoretical and experimental result is a poor modeling of the outer shells of the Thomas-Fermi atoms within our numerical method. This assertion is supported by Fig. 1 where the cluster looks just as a collection of independent individual isolated atoms.

Fortunately in our approach we can freely tune the width of the central gaussian (parameter ξ) thus continuously interpolating between two limiting cases. In the first case (studied in the previous section) of small values of ξ the core electrons are perfectly modeled whereas the outer shell is not. In the opposite case of large ξ, the quality of outer shell modeling significantly increases at the cost of poorer modeling of the core electrons, which, however, do not play any role in the energy absorption in the considered regime.

Therefore we decided to try the case where the half (nine in our case) of the atom electrons is frozen and the remaining half is free to move around. It looks reasonable as in the experiment each atom looses two electrons at average. Notice please, that in a recent theoretical paper dealing with xenon [19] only the ionized electrons were allowed to move and the rest were attached to the nucleus, forming an effective Yukawa scattering potential.

This weak absorption should be contrasted with the behavior presented in Fig. 8. In this figure we plot the total absorbed energy measured in photons per atom as a function of time. The calculations are done for $\xi = 0.5$ and two different cluster sizes of $N = 55$ (the ground state of this cluster is depicted in Fig. 2) and $N = 147$ atoms. The absorbed energy increases with the size of the cluster and reaches the experimental result of 20 photons per atom already for a 147 atom cluster. The decrease in the energy absorption speed after the maximum of the pulse visible for the 55 atoms case corresponds to the destruction of collective electron oscillations by the cluster explosion.

Let us mention that the energy oscillations seen in Fig. 8 for the case of 147 atoms are of purely numerical origin. The tree-based multipole method [50–53] of calculating the Coulomb force has to deal with multiple scales of the system. It has to properly model both the individual ions and the cluster as a whole. When the size of the system becomes sufficiently large energy oscillations appear. We have checked that they persist also for a smaller time step. Note however that these oscillations are small with respect to the absolute value of cluster energy (c.f., Fig. 3).

In Fig. 5 we plot the resulting distribution of the final charges of the ions formed in the explosion of the 55 atoms cluster from Fig. 2 illuminated by a short-wavelength pulse. The result of average ionization degree of two electrons per atom matches well the experimental result [18].

In Fig. 10 we present the structure of the cluster just after the pulse is finished. It shows that the atoms from the outer shells started to move. Still the atoms of the cluster stay together - the pulse itself was not able to totally disintegrate the cluster what is the case for optical frequencies. Although the electron cloud excited by the pulse is still well within the spatial structure of the cluster it already starts to affect the atoms forming the inner shells of the cluster. This could lead in principle to collisional ionization.

Another possible ionization mechanism is field ionization by the strong Coulomb field of the ions inside the cluster. Indeed an inset to Fig. 10 shows the electron

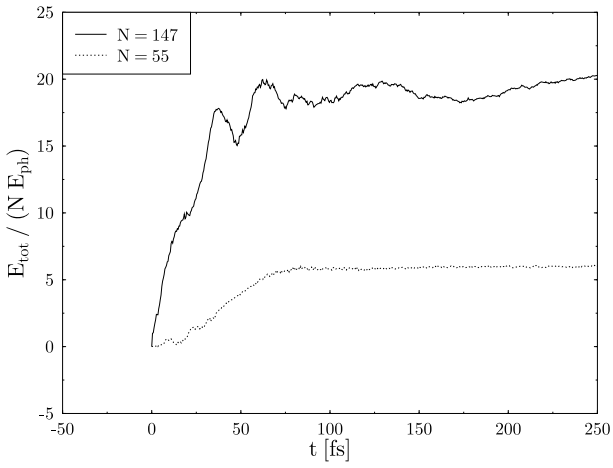

FIG. 8: Total energy absorbed by clusters of different sizes subjected to short-wavelength laser pulse plotted as a function of time. The results are presented in average number of photons absorbed per atom. The energy acquired by the cluster increases strongly with its size.

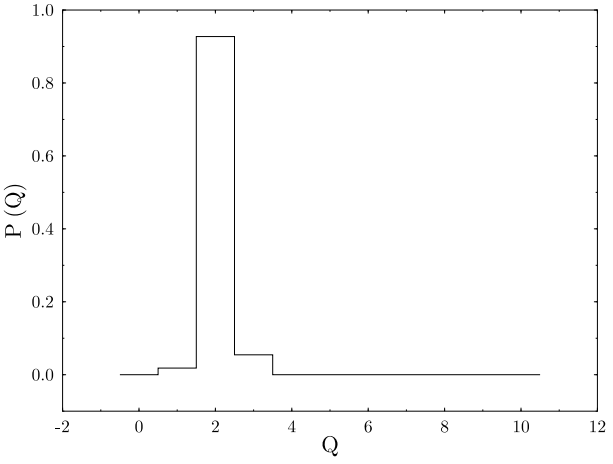

FIG. 9: Distribution of the final charges of the ions formed in the explosion of an 55 atom cluster.

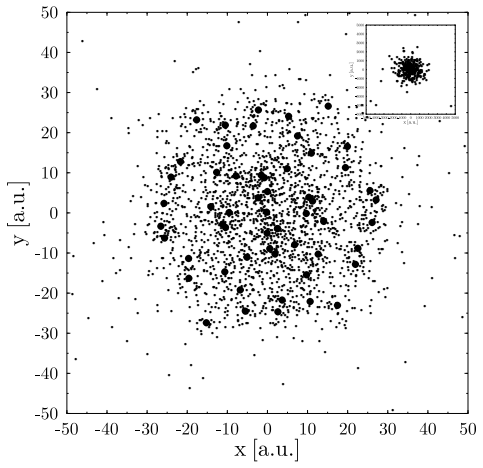

FIG. 10: Excited $N = 55$ atom cluster from Fig. 2 at the end of the free-electron laser pulse at $t = 100$ fs. Positions of the nuclei $\{\vec{R}_a\}$ are marked by filled circles. Small black dots correspond to the positions of the pseudo-particles modeling the electronic density ρ. An inset shows the electron cloud at a $1 : 100$ magnification (i.e., the x and y coordinates vary from -5000 to 5000 [a.u.]. The size of the cluster is only about two times larger than the ground state structure from Fig. 2.

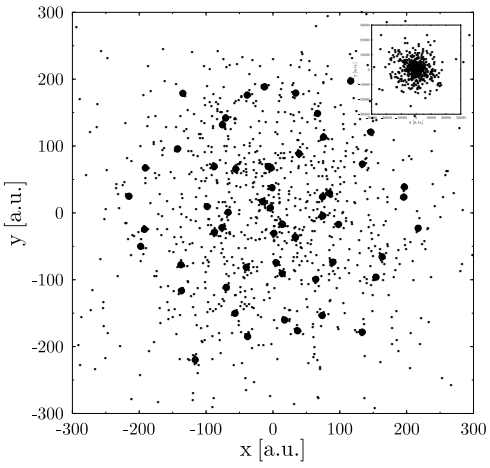

FIG. 11: Excited $N = 55$ atom cluster with $\xi = 0.5$ at $t =$ 700fs.

cloud at a $1 : 100$ magnification. Most of the electrons remain still to be bound by the cluster as whole but the size of this bound electron cloud is much larger than the size of the cluster. Thus the cluster core becomes positively charged what leads to production of the highly charged ions at the cluster surface. That it is indeed the case will be seen in the forthcoming figures.

In Fig. 11 we see the cluster structure after longer time, namely seven times as long as in the previous case. The cluster behavior is thus influenced by the period of "without-the-pulse" evolution. The outer shell is apparently moving away from the cluster but the atoms from the deeper located shells are still close to each other. They continue, however, to be ionized by the excited electrons. The inset to Fig. 10 illustrates an isotropic character of the explosion (remember that the electric field of the laser pulse was polarized along the x axis).

As seen from Fig. 11 the cluster size is comparable with the optical case depicted in Fig. 4. There are still some electrons inside the cluster structure but the energies and charges of the ions do not practically change if we further propagate the cluster in time. Thus in Fig. 12 we have the kinetic energy of the ions plotted as a function of the charge state. Both charges and energies were calculated at $t = 700$fs. As opposed to the optical case from Fig. 6 now the ions with higher charges come from the outer shells of the cluster. As already mentioned, one possible explanation of this result is the influence of the Coulomb field of the cluster core. It lowers the ionization potential

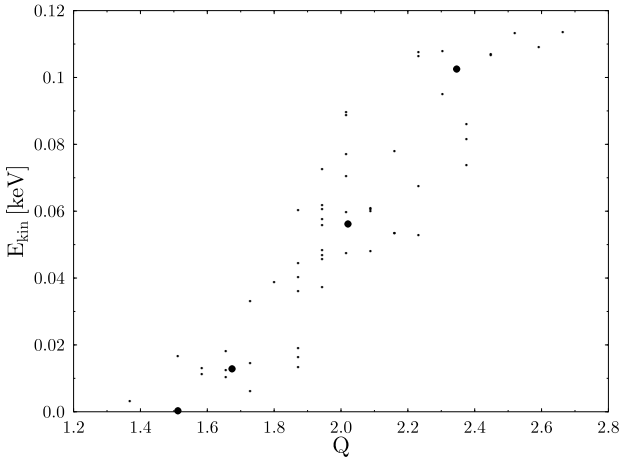

FIG. 12: Kinetic energy of the ions plotted as a function as the charge state in the short-wavelength case. Small dots correspond to individual ions while larger filled circles represent results averaged over (sub)shells.

for the ions from the outer shells of the cluster facilitating their ionization.

Last but not least let us mention that a straight line seems to be a good approximation for the functional dependence from Fig. 12. This could indicate a hydrodynamic explosion scenario [1, 7] for the short-wavelength pulse.

VI. BRIEF SUMMARY

Using a rather simplified yet powerful approach we have addressed a "hot" topic in the field of cluster physics, namely, that of the rare-gas atomic clusters explosion driven by a short X-ray pulse absorption. Despite its simplicity our time-dependent Thomas-Fermi model happened to provide quite realistic description of both the ionization and explosion processes. Using the pulse parameters of the actual experiments we have obtained quite impressive qualitative agreement with the measured quantities.

Let us stress that our simple unified model encompasses two different cases and, surprisingly enough, enables us to track down two different physical mechanisms responsible for the explosion dynamics in both considered regimes. It seems that in the realm of optical frequencies the electrons are released mainly by external laser field (above-the-barrier ionization process). The static electric fields of the other ions play only a minor role in lowering the ionization barrier. The released electrons are driven to move back and forth along the polarization axis of the laser wave. We suspect that they cause inner shell atoms to be more ionized that those from outer shell. The physical reason for that could be the fact that due to Coulomb expansion of the ions, the inner shell atoms are more likely to be hit by the moving electrons.

In the ultraviolet regime, the physical mechanism seems to be different. First of all, the pulse do not directly ionize the atoms but rather excite the electrons. As a result the electron cloud expands isotropically still being bounded by cluster as a whole. As a natural consequence, the inner part of the cluster becomes positively charged and resulting Coulomb field lowers the ionization barrier facilitating ionization of atoms, especially that of the outer shells.

It also seems that our model is able to reproduce the strong energy absorption observed in the experiment and, beyond that, provides a framework for explaining and interpreting this phenomenon. Moreover the nonlinearity inherent in our model allows us to look further towards even stronger intensity regimes. This line of development will be pursued in a forthcoming paper.

Acknowledgment

This work was supported by the Polish Committee for Scientific Research (KBN) under Grant No. 5 P03B 063 20.

[1] T. Ditmire, T. Donnelly, A. M. Rubenchik, R. W. Falcone, and M. D. Perry, Phys. Rev. A **53**, 3379 (1996).

[2] A. McPherson, B. D. Thompson, A. B. Borisov, K. Boyer, and C. K. Rhodes, Nature **370**, 631 (1994).

[3] A. McPherson, T. S. Luk, B. D. Thompson, A. B. Borisov, O. B. Shiryaev, X. Chen, K. Boyer, and C. K. Rhodes, Phys. Rev. Lett. **72**, 1810 (1994).

[4] T. Ditmire, T. Donnelly, R. W. Falcone, and M. D. Perry, Phys. Rev. Lett. **75**, 3122 (1995).

[5] E. M. Snyder, S. A. Buzza, and A. W. Castleman Jr., Phys. Rev. Lett. **77**, 3347 (1996).

[6] M. Lezius, S. Dobosz, D. Normand, and M. Schmidt, J. Phys. B **30**, L251 (1997).

[7] T. Ditmire, J. W. G. Tisch, E. Springate, M. B. Mason, N. Hay, R. A. Smith, J. Marangos, and M. H. R. Hutchinson, Nature **386**, 54 (1997).

[8] M. Lezius, S. Dobosz, D. Normand, and M. Schmidt, Phys. Rev. Lett. **80**, 261 (1998).

[9] Y. L. Shao, T. Ditmire, J. W. G. Tisch, E. Springate, J. P. Marangos, and M. H. R. Hutchinson, Phys. Rev. Lett. **77**, 3343 (1996).

[10] T. Ditmire, J. W. G. Tisch, E. Springate, M. B. Mason, N. Hay, J. P. Marangos, and M. H. R. Hutchinson, Phys. Rev. Lett. **78**, 2732 (1997).

[11] T. Ditmire, Phys. Rev. A **57**, R4094 (1998).

[12] K. Ishikawa and T. Blenski, Phys. Rev. A **62**, 063204 (2000).

[13] I. Last and J. Jortner, Phys. Rev. A **62**, 013201 (2000).

[14] I. Last and J. Jortner, Phys. Rev. Lett. **87**, 033401 (2001).

[15] C. Siedschlag and J. M. Rost, Phys. Rev. Lett. **89**, 173401 (2002).

[16] V. Véniard, R. Taïeb, and A. Maquet, Phys. Rev. A **65**, 013202 (2001).

[17] H. Wabnitz, L. Bittner, A. R. B. de Castro, R. Dohrmann, P. Gurtler, T. Laarmann, W. Laasch, J. Schulz, A. Swiderski, K. von Haeften, et al., Nature **420**, 482 (2002).

[18] T. Laarmann, A. R. B. de Castro, P. Gürtler, W. Laasch, J. Schulz, H. Wabnitz, and T. Möller, Phys. Rev. Lett. **92**, 143401 (2004).

[19] R. Santra and C. H. Greene, Phys. Rev. Lett. **91**, 233401 (2003).

[20] M. Rusek, H. Lagadec, and T. Blenski, Phys. Rev. A **63**, 013203 (2001).

[21] M. Brewczyk, C. W. Clark, M. Lewenstein, and K. Rzążewski, Phys. Rev. Lett. **80**, 1857 (1998).

[22] M. Brewczyk and K. Rzążewski, Phys. Rev. A **60**, 2285 (1999).

[23] M. Rusek and A. Orłowski, Acta Phys. Pol. **105**, 425 (2004).

[24] M. Rusek and A. Orłowski, Acta Phys. Pol. **106**, 3 (2004).

[25] L. H. Thomas, Proc. Camb. Phil. Soc. **23**, 542 (1926).

[26] E. Fermi, Zeit. Phys. **48**, 73 (1928).

[27] P. Hohenberg and W. Kohn, Phys. Rev. **136**, B864 (1964).

[28] W. Kohn and L. J. Sham, Phys. Rev. **140**, A1133 (1965).

[29] L. A. Wittwer and S. D. Bloom, Phys. Rev. A **8**, 2249 (1973).

[30] S. M. Susskind, E. J. Valeo, C. R. Oberman, and I. B. Bernstein, Phys. Rev. A **43**, 2569 (1991).

[31] W. Benz, in *The Numerical Modeling of Nonlinear Stellar Pulsations*, edited by J. R. Buchler (Kluwer, Dordrecht,

1990), pp. 269–288.
[32] J. J. Monaghan, Annual Reviews of Astronomy and Astrophysics **30**, 543 (1992).
[33] L. B. Lucy, Astron. J **82**, 1013 (1977).
[34] R. Gingold and J. Monaghan, Mon. Not. R. astr. Soc. **181**, 375 (1977).
[35] F. Bloch, Z. Phys. **81**, 363 (1933).
[36] J. A. Ball, J. A. Wheeler, and E. L. Fireman, Rev. Mod. Phys. **45**, 333 (1973).
[37] K. Ishikawa, B. U. Felderhof, T. Blenski, and B. Cichocki, J. Plasma Phys. **60**, 787 (1998).
[38] M. Brewczyk, K. Rzążewski, and C. W. Clark, Phys. Rev. A **52**, 1468 (1995).
[39] N. H. March, in *Theory of the inhomogeneous electron gas*, edited by S. Lundqvist and N. March (Plenum Press, New York, 1983), pp. 1–77.
[40] P. Gombas, *Die Statistische Theorie des Atoms und ihre Anwendungen* (Springer, Wien, 1949).
[41] J. Farges, M. F. de Faraudy, B. Raoult, and G. Torchet, J. Chem. Phys. **78**, 5067 (1983).
[42] J. Farges, M. F. de Faraudy, B. Raoult, and G. Torchet, J. Chem. Phys. **84**, 3491 (1986).
[43] J. A. Northby, J. Chem. Phys. **87**, 6166 (1987).
[44] D. Wales and J. Doye, J. Phys. Chem. A **101**, 5111 (1997).
[45] `http://www-wales.ch.cam.ac.uk/~jon/structures/LJ.html`.
[46] E. D. Potter, Q. Liu, and A. H. Zewail, Chem. Phys. Lett. **200**, 605 (1992).
[47] E. Teller, Rev. Mod. Phys. **34**, 627 (1962).
[48] J. Purnell, E. M. Snyder, S. Wei, and A. W. Castelman, Chem. Phys. Lett. **229**, 333 (1994).
[49] M. Brewczyk and K. Rzążewski, J. Phys. B **34**, L289 (2001).
[50] A. W. Appel, SIAM J. Sci. Stat. Comput. **6**, 85 (1985).
[51] J. E. Barnes and P. Hut, Nature **324**, 446 (1986).
[52] L. Greengard, Computers in Physics **4**, 142 (1990).
[53] L. Greengard, Science **265**, 909 (1994).